ChemBioChem

Research Article
doi.org/10.1002/cbic.202300739

Chemistry Europe
European Chemical Societies Publishing

www.chembiochem.org

VIP *Very Important Paper*

Two-Factor Fluorogenic Cyanine-Styryl Dyes with Yellow and Red Fluorescence for Bioorthogonal Labelling of DNA

Bastian Pfeuffer,[a] Philipp Geng,[a] and Hans-Achim Wagenknecht*[a]

An orange- and a red-emitting tetrazine-modified cyanine-styryl dyes were synthesized for bioorthogonal labelling of DNA by means of the Diels-Alder reaction with inverse electron demand. Both dyes use the concept of the "two-factor" fluorogenicity for nucleic acids: (i) The dyes are nucleic-acid sensitive by their non-covalent binding to DNA, and (ii) their covalently attached tetrazine moiety quench the fluorescence. As a result, the reaction with bicyclononyne- and spirohexene-modified DNA is significantly accelerated up to $k_2 =$ 280,000 $M^{-1} s^{-1}$, and the fluorescence turn-on is enhanced up to 305. Both dyes are cell permeable even in low concentrations and undergo fluorogenic reactions with spirohexene-modified DNA in living HeLa cells. The fluorescence is enhanced in living cells to such an extent that washing procedures before cell imaging are not required. Their large Stokes shifts (up to 0.77 eV) also makes them well suited for imaging because the wavelength ranges for excitation and emission can be best possible separated. Furthermore, the spirohexene-modified nucleosides and DNA extend and improve the toolbox of already existing "clickable" dyes for live cell imaging.

Introduction

Tetrazines undergo fast inverse electron-demand Diels-Alder reactions (iEDDA) with second-order rate constants of up to 10^6 $M^{-1} s^{-1}$ for bioorthogonal protein labelling.[1] Compared to other "click" reactions, namely the copper-catalyzed azide-alkyne cycloaddition or the photoclick reactions, the iEDDA reaction as bioorthogonal reaction is extremely fast and does not require cytotoxic metal catalysts, light or any other additive and is therefore the ideal candidate for live cell imaging.[2] Unlike the normal Diels-Alder reaction with an electron-rich diene and an electron-poor dienophile, the iEDDA reaction flips the electronic scenario. Here, a strained dienophile reacts with an electron-poor diene, the tetrazine. The release of nitrogen in the second step of this bioorthogonal reaction is key to get quantitative yields.

Tetrazine-modified dyes effectively link the dye to the desired target biomolecule and improve the signal-to-noise ratio in wash-free cell imaging experiments.[3] Fluorogenic probes are essential also for super-resolution spectroscopy.[4] The fluorescence of the dye is quenched due to the tetrazine moiety. During the iEDDA, the quencher tetrazine is converted to the pyrazine and as a result the fluorescence is released.[5] Many of the results published are for protein labelling and are based on the use of green fluorescent tetrazine-modified dyes. For example, Weissleder *et al.* stained cells with tetrazine-modified BODIPY dyes.[6] However, BODIPY dyes exhibit a small Stokes shift, which makes it difficult to separate excitation and emission wavelengths, and a high degree of photobleaching. *Wombacher et al.* were able to extend the spectrum of fluorescent tetrazine-modified dyes to yellow- and red-emissive representatives of their class based on xanthenes.[7] Red dyes are enormously important for the fluorescent labelling of cells due to their excitation with lower energy light, associated with less stress for the living cell and deeper penetration into tissue. However, these xanthenes showed only small Stokes shifts and only small fluorescence enhancements compared to their green fluorescent derivatives. A systematic study of coumarin-tetrazine turn-on probes was presented by *Vrabel et al.*[8]

Moving the emission of tetrazine-modified dyes into the yellow and red range is a challenge because the fluorogenicity typically drops in these fluoresence ranges.[9] *Kele et al.* recently found out for tetrazine-Cy3 probes, that the close conjugation *via* a vinylene bridge or a single C–C bond between the tetrazine as quencher and the dye is critical for the fluorogenicity.[10] However, both Cy3 and the acridines, the latter recently described as tetrazine conjugates by *Mahuteau-Betzer et al.*, are not fluorescence-sensitive to nucleic acids.[11] Nucleic acid-sensitivity requires a templated pre-binding of the dye as recently evidenced by *Luedtke et al.* for an acridine.[12] In this work, we follow our recently established concept of the "two-factor" fluorogenicity for nucleic acids and present a yellow and a red emitting cyanine-styryl dye for "click" reactions designed for bioorthogonal labelling of DNA by means of strained alkenes and alkynes as DNA modifications (Figure 1). This concept uses the DNA-templated effects to the dye as second factor for fluorogenicity, additional to the tetrazine quenching as first factor for fluorogenicity.[13] In addition to large Stokes shifts, these dyes exhibit red-shifted emission wavelengths of up to approx. 700 nm with extremly fast

[a] *B. Pfeuffer, Dr. P. Geng, Prof. Dr. H.-A. Wagenknecht*
Institute of Organic Chemistry
Karlsruhe Institute of Technology (KIT)
Fritz-Haber Weg 6, 76131 Karlsruhe, Germany
E-mail: hans-achim.wagenknecht@kit.edu

Supporting information for this article is available on the WWW under https://doi.org/10.1002/cbic.202300739

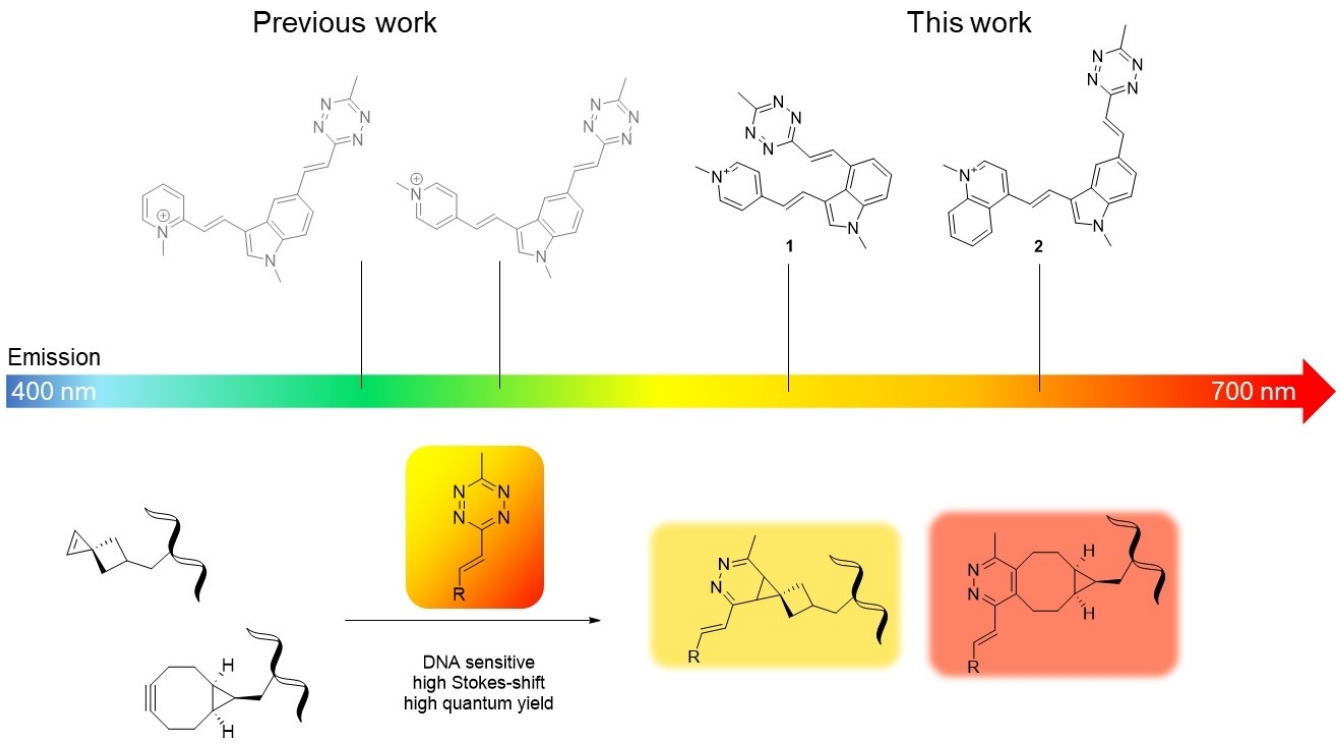

Figure 1. Moving the emission of tetrazine-modified cyanine-styryl dyes into the yellow and red range based on our two-factor fluorogenicity for nucleic acids. Cyanine-styryl dyes are DNA sensitive by their fluorescence, show large Stokes' shifts, good quantum yields, high photostability, high turn-on and extremely fast kinetics behaviour especially with nucleic acids. As reactive counterpart, spiroalkene- and BCN-modified nucleosides and DNA were used.

kinetics. Also they feature high quantum yields as well as high turn on rates. As a click-partner for bioorthogonal labelling in living cells and *in vitro* we synthesized a small library of BCN- and spirohexene-modified nucleosides and DNA. Especially spirohexene-modified nucleosides were used for protein labelling,[14] but to the best of our knowledge, not yet used for bioorthogonal labelling. Compared to cyclopropenes which have wide structural similarities, spiroalkenes combine stability, reactivity and physicochemical properties to extend and improve the toolbox of already existing clickable dyes for live cell imaging.

Results and Discussion

The methyl-substitued tetrazine as both bioorthogonally reacting moiety and quencher was conjugated to the dye core by a vinylene bridge to allow efficient fluorescent quenching in the cyanine styryl dyes **1** and **2** (Scheme 1). For dye **1**, the 4-methylated pyridinium salt **5** was chosen for conjugation with 4-bromoindole **6** to achieve orange emission of the dye. In dye **2**, the 4-methylpyridinium salt was extended by annulation of another phenyl group to form the 4-methylquinolinium salt **7** and conjugated to the 5-bromoindole **8** to accomplish red emission through the extended π-system. The synthesis follows this design approach, and the dye precursors **3** and **4** were accordingly synthesized. The 5-bromoindole **8** reacts with 1,4-dimethylquinolinium (**7**) to the dye precursor **4** and the formylated 4-bromoindole reacts to the dye precursor **3**. Both

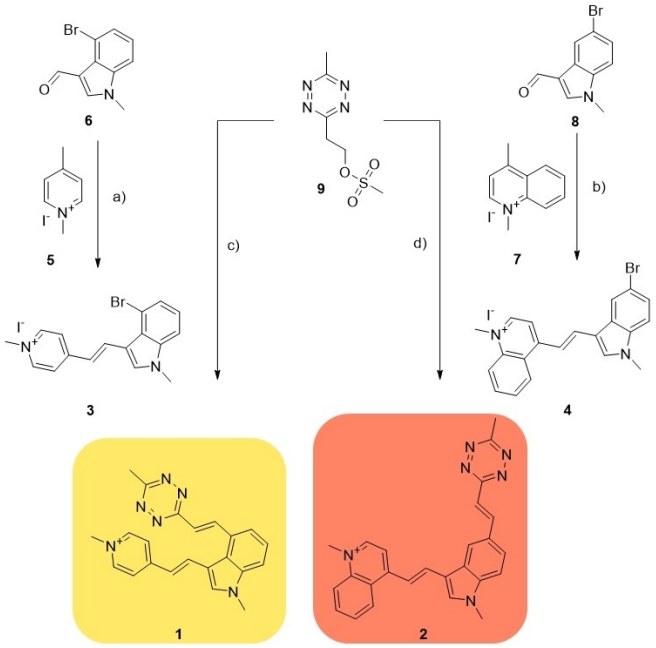

Scheme 1. Synthesis of the dyes **1** and **2** via Heck coupling of the precursors **3** and **4** with tetrazine precursor **9**: a) **6**, EtOH, **5**, piperidine, 16 h, 80 °C, quant., b) **7**, EtOH, **8**, piperidine, 16 h, 80 °C, 95 %, c) **3**, $Pd_2(dba)_3$, QPhos, DMF, **9**, Et_3N, 18 h, 100 °C, 31 %, d) **4**, $Pd_2(dba)_3$, QPhos, DMF, **9**, Et_3N, 18 h, 80 °C, 13 %.

dye precursors, **3** and **4**, were obtained in good yields of 79 % and 88 %, respectively, over two steps. Finally, the mesylated

tetrazine **9** was conjugated with the dyes **3** and **4** by adapting a method from Kele *et al.*[14] We used a heating block to heat the solutions of substrate **3** and **4**, respectively, to 100 °C in crimp vials under argon atmosphere. We obtained pure products with 31 % for **1** and 13 % yield for **2**.

As a click-partner for bioorthogonal labelling in living cells and *in vitro* we synthesized a small library of BCN- and spirohexene (SPH)-modified nucleosides (Scheme 2) and DNA (Scheme 3). In addition to varying the type of DNA base, uracil (**12**, **13**, **16** and **17**) or adenine (**14**, **15**, **18** and **19**), we wanted to investigate the impact of two different linkages, either flexible (propynyl) and rigid (propyl), to elucidate their potential influence on the fluorescence turn-on values and on the kinetics of the iEDDA reaction. We assume that the additional 2′-hydroxyl group at the uridines **12**, **13**, **16** and **17** can be excluded due to the large spatial separation from the reactive

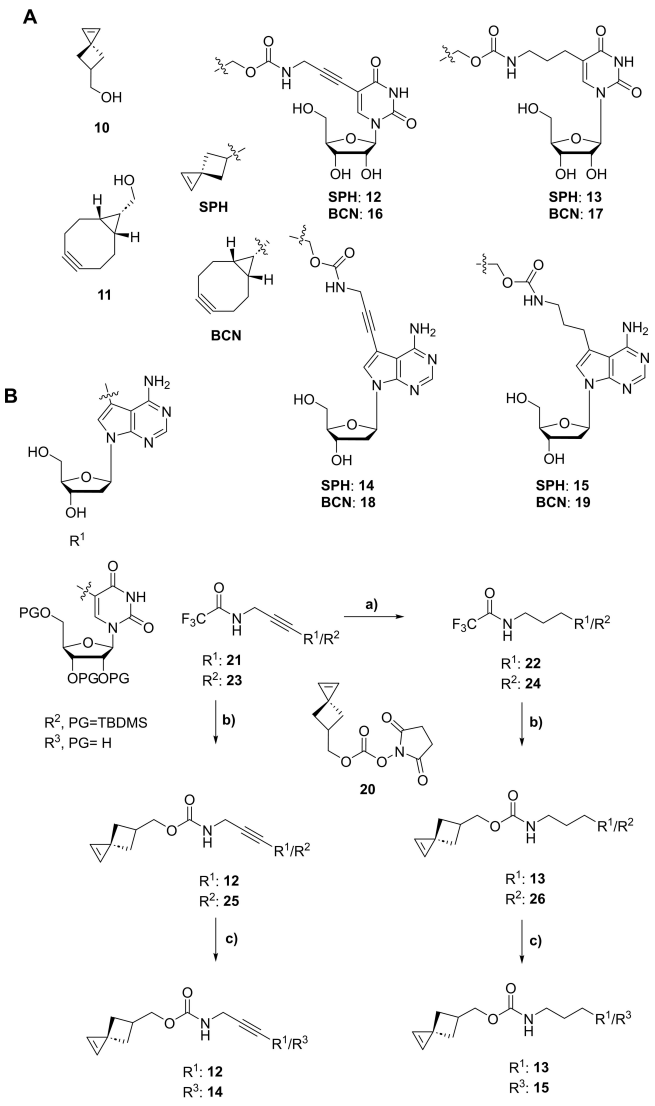

Scheme 2. A) SPH- and BCN-modified uridines **12**/**13** and **16**/**17**, and 2′-deoxyadenosines **14**/**15** and **11**/**12**. B) Synthesis of the SPH-modified uridines **12**/**13** and 2′-deoxyadenosine **14**/**15**: a) MeOH, H_2, Pd/C, 7 h, r.t., quant., b) NaOH, MeOH, r.t., 2 h, Et_3N, DMF, 16 h, r.t., **20**, **14**: 20 %, **15**: 33 %, **25**: 72 %, **26**: 38 % c) $Et_3N \cdot 3HF$, THF, r.t., 18 h, **12**: 70 %, **13**: quant.

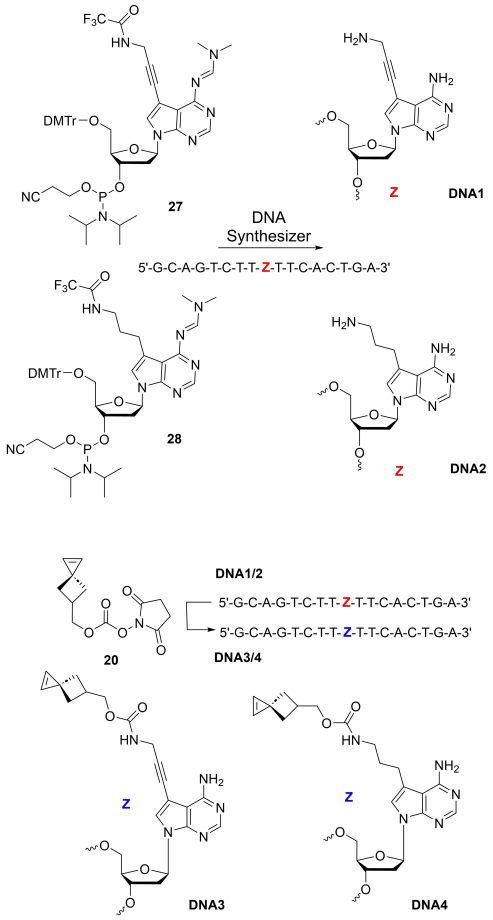

Scheme 3. Synthesis of the SPH-modified **DNA3**-**DNA4** starting from phosphoramidite **27** and **28** *via* solid phase synthesis with postsynthetic modification of **DNA1**-**DNA2**.

group. The BCN-modified uridines **16**/**17** and the 2′-deoxyadenosines **18**/**19** were synthesized according to literature.[13] The SPH-modified uridines **12**/**13**, and the 2′-deoxyadenosines **14**/**15** require the spirohexene NHS ester **20** as starting material that was synthesized following a synthetic route published by *Lin et al.*[15] The coupling of the NHS ester **20** to the uridine and 2′-deoxyadenosine precursors **21**–**24** were performed analoguos to the protocols for the BCN-modified ones (Figure S46 and S47).

Time-dependent fluorescence measurements allowed the precise investigation of the reaction progress to determine the resulting enhanced fluorescence by the turn-on value tov and the second-order rate constant k_2 (Figure 2). The simple reactive alcohols, **10** and **11**, show only very low turn-on values in the range of tov = 2–6 and slow kinetics with constants in the range of $k_2 = 0.6–3\ M^{-1}s^{-1}$. In contrast, the modified nucleosides show higher turn-on values by a factor 3–10 for the SPH-modified **12**–**15** (see Table 1) and by a factor of 2–6 for the BCN-modified nucleosides **16**–**19**, to tov of 31 and 32, respectively. This is primarily due to increased steric hindrance, which has a significant impact on quenching the fluorescence of the fluorophore. However, the difference of the linkers is not as significant as the difference between 7-deaza-2′-deoxyadeno-

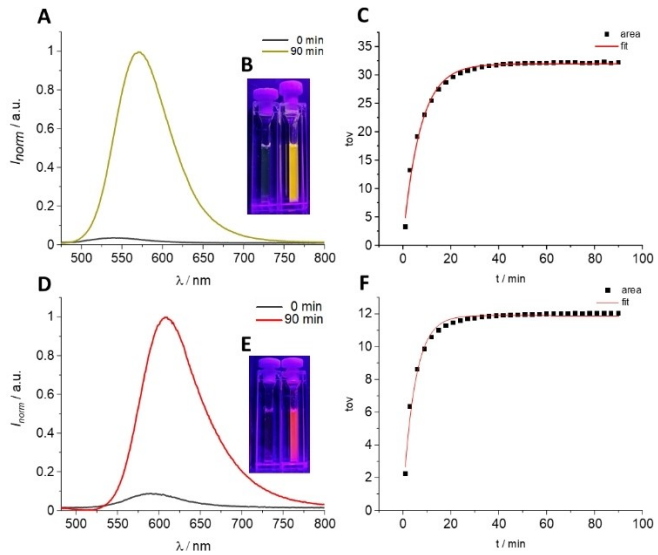

Figure 2. A) Increase of fluorescence intensity (λ_{exc} = 423 nm) during the reaction of nucleoside **14** (100 μM, 5.00 equiv.) with dye **1** (20 μM) in H_2O with 1% DMSO. B) Visible turn-on effect: **1** before (left cuvette) and after the reaction with **14** (right cuvette). C) Kinetic plot with of tov against time the exponential fit function y = a + b·exp(−k·x). D) Increase of fluorescence intensity (λ_{exc} = 467 nm) during the reaction of **14** (100 μM, 5.00 equiv.) with **2** (20 μM) in H_2O with 1% DMSO. E) Visible turn on effect: **2** before (left) and after reaction with **14** (right). F) Kinetic plot of tov against time with exponential fit function y = a + b·exp(−k·x). For kinetic measurements and turn-on values of other ractions, see SI Figure S11–S44.

Table 1. Table of all tov, quantum yields (Φ_F) and k_2 of **10**–**19** and **DNA3**-**dsDNA6** with **1** + **2**.

	1 tov	**1** Φ_F	**1** $k_2/M^{-1}s^{-1}$	**2** tov	**2** Φ_F	**2** $k_2/M^{-1}s^{-1}$
10	4	0.004	0.60	2	0.003	2.65
11	6	0.008	3.00	3	0.005	1.80
12	19	0.005	5.4	18	0.003	6.7
13	23	0.004	2.5	14	0.004	4.3
14	31	0.004	13.4	12	0.003	24.0
15	20	0.003	11.9	6	0.004	12.0
16	12	0.013	64.0	16	0.018	28.6
17	32	0.029	28.0	14	0.017	14.7
18	10	0.011	500	16	0.022	267
19	26	0.021	152	7	0.011	88.0
DNA3	130	0.020	n.d.[a]	60	0.018	n.d.[a]
DNA4	89	0.016	n.d.[a]	42	0.012	n.d.[a]
dsDNA3	251	0.040	n.d.[a]	90	0.042	n.d.[a]
DNA5	70	0.040	280000	115	0.160	63000
DNA6	104	0.050	203000	159	0.150	124000
dsDNA5	222	0.160	99000	305	0.150	73000
dsDNA6	138	0.190	138000	235	0.125	67000

[a] Not determined, see text.

sine and uridine. For the SPH-modified nucleosides we achieved the highest tov of 31 with **14**+**1**. For the BCN-modfied nucleosides **16**–**19**, we obtained the highest turn on value of tov = 32 for the reaction of **17** with **1**, with the flexible propynyl linker, whereas the rigid propyl linker yielded better turn-on values of tov = 16 for the reaction of **18** with **2**. In both cases, we achieved similar results in kinetic studies, as we obtained a faster reaction rate for the 2′-deoxyadenosines **18** with **1** of up to 500 $M^{-1}s^{-1}$ (Figure 3). The formation of all "click" products **29**–**48** was followed by fluorescence spectroscopy (Figures S11–S44).

After comparing these results, we concluded that the 7-deaza-2′-deoxadenosines are best suited for further experiments with modified DNA, since they react very selectively with turn-on values of tov = 31 and 26, for **14** + **1** and **19** + **1**, respectively, and a second-order rate constant of k_2 = 24 $M^{-1}s^{-1}$ and 500 $M^{-1}s^{-1}$ for **14** + **2** and **18** + **1**, respectively. Since both linker types worked very well in those experiments with nucleosides, we decided to synthesize DNA with both linker types in order to facilitate a more comprehensive comparison within the cellular experiments. We synthesized the BCN- and SPH-modified **DNA3**-**DNA6** using the phosphoramidite **27** and **28** for standard solid-phase and automated DNA synthesis, and postsynthetic modification with the NHS esters **20** and **49**. The synthesis of the BCN-modified **DNA5**-**DNA6** was published,[13]

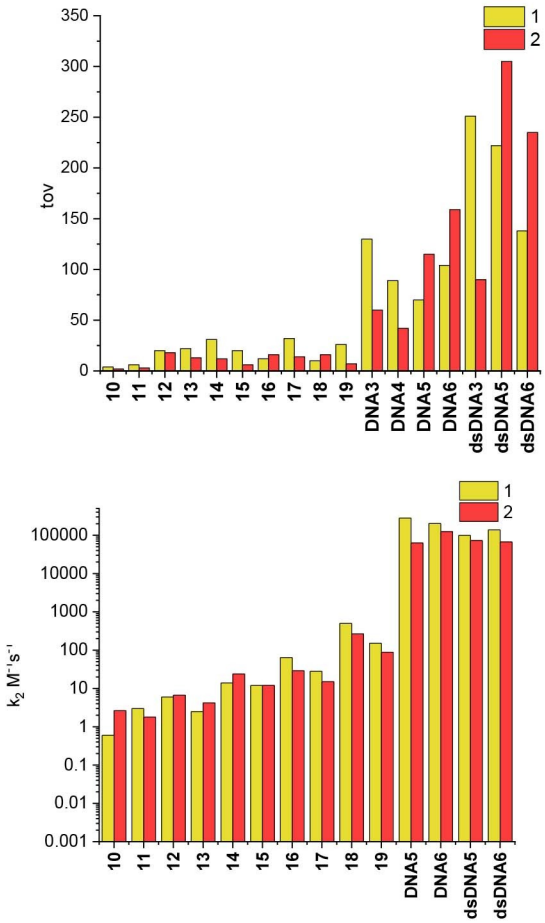

Figure 3. Comparison of the turn on values tov and second-order reaction constants for the reaction of the alcohols, uridines and 2′-deoxyadenosines **10**–**19** and **DNA3**-**dsDNA6** with **1** + **2**.

the synthesis of the SPH-modified **DNA3**-**DNA4** was done similarly (see Experimental Section).

For the labelling experiments, significantly smaller quantities of DNA strands were available, that the reaction volumes had to be adjusted accordingly. The concentrations were diluted by a factor of 1:10. In order to ensure comparability with the nucleoside experiments described above, the ratio of 1:5 between the fluorophore and dienophile was maintained at such lower concentrations. Interestingly, a complete conversion to the labelled DNA products was observed after only three seconds for the BCN-modified **DNA5** and **DNA6**. This yields a reaction constant of $k_2 = 1.24 \cdot 10^5\ M^{-1}s^{-1}$ for the **DNA6**, modified with BCN via the flexible propyl linker, with **2**, and $k_2 = 2.80 \cdot 10^5\ M^{-1}s^{-1}$ for the BCN-modified **DNA5**, also modified with BCN but via the rigid propyl linker, with **1**, respectively. Also the turn on values raised up to tov = 159 for **DNA6** with **2**, and tov = 104 for **DNA6** with **1**. Once again, the increase in kinetics and turn on values were likely due to the increased steric demand of the DNA compared to the nucleosides. Additionally, we assume a DNA-templated pre-coordination of the dyes to the DNA due to electrostatic attraction of the positively charged dye and the negatively charged DNA as we evidenced previously.[11] A clear increase in the turn on effect was also observed with the SPH-modified DNA. However, no reaction rate constants could be determined. Due to the smaller reactive species (SPH), we suspect that the SPH-modified **DNA3**-**DNA4** are tighter coiled and could therefore not react with the tetrazine-dyes **1** and **2** at room temperature. We presume this because of the low turn-on values immediately after mixing, which can be almost exclusively attributed to the non-covalent pre-coordination of the dye with the DNA. Additionally, no reaction progress was observed after a few hours at room temperature. However, by warming up the DNA samples in the presence of the dyes **1** and **2** to 60 °C, a significant increase in fluorescence was detected. We suspect that the heat causes denaturing of the DNA, allowing the diene and the dienophile to react with each other. In contrast to the nucleosides **14** and **15**, there is also a significantly enhanced turn on of tov = 42 and 60 for **DNA3** and **DNA4** with **2** and tov = 89 and 130 for the reaction with **1**, respectively. Finally, we annealed the BCN- and SPH-modified oligonucleotides **DNA3** and **DNA5** by their complementary counterstrands to double-stranded DNA to **dsDNA3** and **dsDNA5**. For the SPH-modified DNA, only the DNA modification with the rigid propyl linker was applied. Strongly increased turn on values were observed, which are significantly higher than those of the corresponding single-stranded DNA of up to = 305 for **dsDNA5** with **2** and tov = 251 for **dsDNA3** with **1**. This further supports our concept of the two-factor fluorogenicity. The high turn-on values and fast kinetics is the prerequisite for the following *in vivo* labelling in cells. The quantum yields of dyes **1** and **2** conjugated with **dsDNA3** are $\Phi_F = 0.04$ which yields brightnesses of $B = 840–920\ M^{-1}cm^{-1}$. The values are higher with the BCN-modified **dsDNA6**, $B = 2738–4009\ M^{-1}cm^{-1}$ because the quantum yields of the conjugates with dyes **1** and **2** are higher, $\Phi_F = 0.125–0.19$. We representatively measured the photostability of the conjugates **DNA3** and **DNA4** during constant and strong irradiation with a 405 nm LED for dye **1** and with a 450 nm LED for dye **2**. Under these rather harsh conditions, dye **1** showed half-lifetimes of $\tau = 21–23$ min, and dye **2** of $\tau = 50–60$ min. These are sufficient photostabilities for the imaging studies.

To demonstrate the bioorthogonality of the described iEDDA reactions and the live-cell imaging under wash-free conditions, HeLa cells were treated and transfected for 24 h with 75 nM of **DNA3** and **DNA5**, respectively, using lipofectamin as transfection reagent. Afterwards, the cells were treated with 150 nM of either dye **1** or **2** for 60 min at 37 °C and imaged via confocal fluorescence microscopy (Figure 4). Without an additional washing step, the "click" product could be clearly visualized inside the cells. Both modified single-stranded DNAs were successfully visualized *in living cells* after reaction with the cyanine-styryl dyes **1** and **2**. In these experiments, SPH-modified **DNA3** exhibited superior performance compared to BCN-modified **DNA5**. This was evident because of the significantly higher produced fluorescence, leading to a more noticeable difference for the fluorescence readout between the negative control (dye only, without prior transfection of cells by modified DNA) and the "clicked" cells. As described for the experiments *in vitro*, heat is required for the rapid conversion of the spirocycle with the tetrazine. The ambient temperature of 37 °C during the 60 min exposure to the cells appears to be sufficient

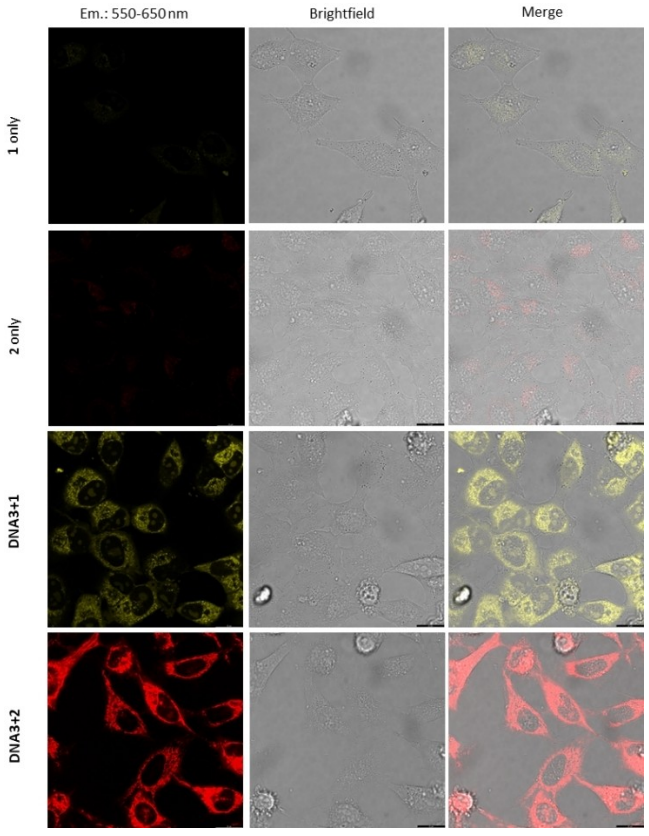

Figure 4. HeLa cells after 24 h transfection with **DNA3** (75 nM) and subsequent labelling with dye **1** and **2** for 60 min. Cells were treated only with **1** and **2** for negative control (top). Imaging by confocal fluorescence microscopy with a 488 nm laser line and an emission of 550–600 nm for experiments with **1** and 600–650 nm for experiments with **2**, complemented with a brightfield channel. Scale bar: 20 μm.

for a visible reaction of the reactive groups. As negative control, we treated HeLa cells only with 150 nM dye **1** or **2** without a transfection of any DNA in advance. No fluorescence signal could be detected in this experiment. Thus, we can be sure that the detected fluorescence signal can be exclusively assigned to the iEDDA reaction products. Due to the low signal-to-noise ratio and the large Stokes shift, no washing step is required to remove the excess of these dyes. Taken together, these features make the dyes **1** and **2** an interesting tool for future cell imaging and metabolic labelling experiments.

In the previous experiments, it was shown that the tetrazine-modified fluorophores **1** and **2** are membrane-permeable. In addition, the iEDDA labellings were successfully carried out with BCN- and SPH-modified DNA in living HeLa cells and the cell images were taken without a subsequent washing step. It looked therefore reasonable to evaluate finally, whether the fluorophores **1** and **2** are able to react with metabolically incorporated modified nucleosides in HeLa cells. 5-Vinyl-2′-deoxyuridine (**VdU**) was chosen for these cell experiments, because it shows excellent incorporation efficiency into genomic DNA, although the iEDDA reaction is slow.[16] After incubation of the fluorophores, the cells were imaged by fluorescence microscopy without subsequent washing steps (Figure 5). The tetrazine-modified fluorophores **1** and **2** were added after the HeLa cells had been fixed. As negative control HeLa cells that were not incubated with **VdU** were also treated with **1** and **2**. Remarkably, the cell images showed the successful labelling of **VdU**-containing genomic DNA by both dyes, **1** and **2**.

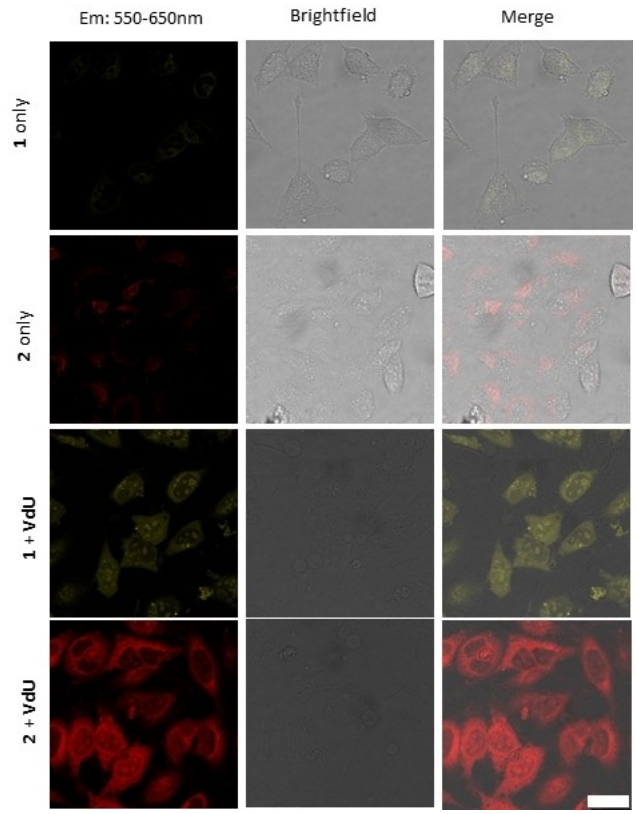

Figure 5. HeLa cells after 24 h transfection with **VdU** (250 μM) and subsequent labelling with dye **1** and **2** for 40 min. Cells were treated only with **1** and **2** for negative control (top). Imaging by confocal fluorescence microscopy with a 488 nm laser line and an emission of 550–600 nm (with **1**) and 600–650 nm (with **2**), complemented with a brightfield channel. Scale bar: 30 μm.

Conclusions

In conclusion, we developed two tetrazine-modified cyanine-styryl dyes, **1** and **2**, that show significant fluoregenicity with both BCN- and SPH-modified DNA. Their significant fluorescence turn-on resulting from the iEDDA reactions allowed to determine the second-order rate constants simply by following the fluorescence changes. A significant enhancement in fluorescence turn-on and acceleration of the reaction kinetics was achieved from the simple functional group alcohols, **10** and **11**, to the BCN- and SPH-modified nucleosides **12**–**19**. By varying the nucleobase (uracil vs. 7-deazaadenine) and the linker (propyl vs. propynyl), the influences of these structural motifs on the efficiency of fluorescence turn-on and reaction rates were determined; values of up to $k_2 = 500\ M^{-1}s^{-1}$ (**18** + **1**) and tov = 32 (**17** + **1**) and tov = 31 (**14** + **1**) were achieved. The reactions are further accelerated by using BCN-modified single-stranded and double-stranded DNA. Remarkably high reaction rate constants of up to $k_2 = 280{,}000\ M^{-1}s^{-1}$ (**DNA5** + **1**) and turn on values of up to tov = 305 (**dsDNA5** + **2**) and 251 (**dsDNA3** + **1**) were determined. The kinetics of the SPH-modified DNA could not be determined because this requires to heat up for full conversion that influences the fluorescence intensity. We assume, however, similar accelerations and enlargements of the fluorescence turn-on based on the experiments with BCN-modified DNA. Nevertheless, a clear correlation between the structure of the different modifications and the iEDDA reaction with tetrazine-modified fluorophores and a two-factor fluorogenicity was observed. Experiments in living HeLa cells have shown that the dyes **1** and **2** are cell permeable and undergo iEDDA reactions with different modified DNA strands and are stable in cellular environment. This concept allows imaging of DNA in living cells with a low signal-to-noise ratio without additional washing steps which is important for cell imaging microscopy and makes it a useful tool for future metabolic labelling experiments. Their large Stokes shifts (up to 0.77 eV) also make them well suited for imaging because the wavelength ranges for excitation and emission can be best possible separated. Furthermore, we showed that SPH-modified nucleosides and DNA extend and improve the toolbox of already existing "clickable" dyes for live cell imaging which was more efficient in our studies than the BCN-modified DNA.

Experimental Section

Materials: All starting materials were obtained from commercial suppliers (Sigma-Aldrich, Fluka, Merck, Alfa Aesar) and used without further purification. All reactions were carried out under a dry argon environment. All solvents were of reagent grade and used as

received. Chemicals and reagents were used as commercially supplied without any further purification unless otherwise stated. Room temperature refers to ambient temperature (20–22 °C). Reactions were monitored by thin layer chromatography (TLC) using aluminum backed silica gel 60 (F254) plates, visualized using UV254 nm and 365 nm and potassium permanganate dips as appropriate. Column chromatography was carried out using silica gel G60 (Fluka analytical, 230–400 mesh, 40–63 μm particle size, 60 Å) as the stationary phase. HeLa cells were bought ATCC (Manassas Virginia).

NMR spectroscopy: ^{1}H and ^{13}C NMR spectra were recorded on a Bruker Ascend 400 MHz spectrometer and a Bruker 500 MHz spectrometer. Chemical shifts are reported in δ units, parts per million (ppm) downfield from TMS. Coupling constants (J) are reported in Hertz (Hz) without adjustments; therefore, due to limits in digital resolution, in some cases there are small differences (< 1 Hz) in the measured J value of the same coupling constant determined from different signals. Splitting patterns are designed as follows: s – singlet, d – doublet, t – triplet, dd – doublet of doublets, dt – doublet of triplets, td – triplet of doublets, ddd – doublet of doublet of doublets, tt – triplet of triplets, sp – septet, hept – heptet, m – multiplet, br – broad. Various 2D techniques experiments were used to establish the structures and to assign the signals.

Mass spectrometry: High-resolution mass spectra were obtained with an electrospray ionization Thermo Exactive orbitrap mass spectrometer. Some of mass spectra were also measured on a Shimadzu Axima Confidence using 3-hydroxypicolinic acid as matrix substance.

Optical Spectroscopy: Spectroscopic measurements were carried out on a Cary 100 Scan UV/vis spectrometer by Varian and a Fluoromax-4 spectrofluorometer by Horiba Jobin-Yvon.

Oligonucleotide synthesis: Oligonucleotide synthesis was performed on a H-6 synthesizer by K&A Laborgeräte. After cleavage, the oligonucleotides were purified by a standard Glen Gel-Pak™ desalting protocol. The purified DNA was used for the post-synthetic BCN coupling and purified on a semi-preparative reversed-phase HPLC ThermoFisher system (RP-C18 column, A = NH_4HCO_3 buffer, B = acetonitrile). The purified oligonucleotide strands were quantified photometrically using a NanoDrop ND-1000 spectrometer.

4: 1,4-Dimethylchinolinium iodide (**7**) (1.10 g. 3.86 mmol, 1.00 equiv.) was placed in a round bottom flask under an argon atmosphere and suspended in EtOH (40 mL). The suspension was stirred for 10 min. **8** (1.38 g, 5.79 mmol, 1.50 equiv.) and piperidine (1.91 mL, 19.3 mmol, 5.00 equiv.) were added to the suspension and stirred overnight at 80 °C. After the reaction mixture had cooled to r.t., Et_2O was added until no more solid precipitated. The precipitate was washed three times with diethyl ether and dried *in vacuo* to obtain a green powder (1.85 g, 95 %). ^{1}H-NMR (400 MHz, DMSO-d_6): δ = 9.10 (d, *J* = 6.4 Hz, 1H, arom.), 8.89 (d, *J* = 8.4 Hz, 1H, arom.), 8.52–8.39 (m, 3H, arom., R–CH=CH–R), 8.33 (s, 1H, arom.), 8.28 (d, *J* = 8.8 Hz, 1H, arom.), 8.22–8.13 (m, 1H, arom.), 8.02–7.88 (m, 2H, arom., R–CH=CH–R), 7.50 (d, *J* = 8.6 Hz, 1H, arom.), 7.39 (d, *J* = 8.5 Hz, 1H, arom.), 4.42 (s, 3H, R–CH_3), 3.88 (s, 3H, R–CH_3). ^{13}C-NMR (101 MHz, DMSO-d_6): δ = 153.2, 146.5, 138.6, 136.4, 136.1, 135.2, 134.5, 128.4, 128.1, 126.0, 125.4, 125.3, 122.0, 118.9, 114.4, 113.8, 113.7, 112.9, 43.9, 33.6. HR-ESI-MS (m/z): $[M]^+$ calcd. for $C_{21}H_{18}N_2Br^+$: 377.0648; found: 377.0651.

3: 1,4-Dimethylchinolinium iodide (**5**) (0.329 g. 1.40 mmol, 1.00 equiv.) was placed in a round bottom flask under an argon atmosphere and suspended in EtOH (40 mL). The suspension was stirred for 10 min. **6** (0.50 g, 2.10 mmol, 1.50 equiv.) and piperidine (0.69 mL, 7.00 mmol, 5.00 equiv.) were added to the suspension and stirred overnight at 80 °C. After the reaction mixture had cooled to r.t., Et_2O was added until no more solid precipitated. The precipitate was washed three times with diethyl ether and dried *in vacuo* to obtain a orange powder (0.637 g, quant.). ^{1}H-NMR (400 MHz, DMSO-d_6): δ = 8.75 (d, *J* = 16.0 Hz, 1H, R–CH=CH–R), 8.68 (d, *J* = 6.7 Hz, 2H, arom.), 8.34 (s, 1H, arom.), 8.00 (d, *J* = 6.7 Hz, 2H, arom.), 7.62 (d, *J* = 8.2 Hz, 1H, arom.), 7.43 (d, *J* = 7.5 Hz, 1H, arom.), 7.19 (t, 1H, arom.), 7.18 (d, *J* = 16.1 Hz, 1H, R–CH=CH–R), 4.21 (s, 3H, R–CH_3), 3.91 (s, 3H, R–CH_3). ^{13}C-NMR (101 MHz, DMSO-d_6): δ = 153.0, 144.6, 138.5, 133.4, 132.5, 125.5, 124.0, 123.5, 122.0, 117.9, 113.0, 112.4, 110.9, 46.5, 33.6. HR-ESI-MS (m/z): $[M]^+$ calcd. for $C_{17}H_{16}N_2Br^+$: 327.0491; found: 327.0470.

2: Compound **4** (0.120 g, 0.238 mmol, 1.00 equiv.), $Pd_2(dba)_3$ (0.012 g, 0.012 mmol, 5 mol %) and QPhos (0.032 g, 0.046 mmol, 20 mol %) were added to a 10 mL crimp-vial and dried under high vacuum. The solids were then solved with dry DMF (1.00 mL). Subsequently, 1.00 mL of a 0.24 M tetrazine stock solution (**9**). and dry Et_3N (0.10 mL, 0.714 mmol, 3.00 equiv.) were added to the solution. The reaction took place in a metal heating block at 100 °C for 18 h. After the solution has cooled to r.t., the solution was mixed with an excess of an aqueous solution of KPF_6 and stirred vigorously for 15 min. The organic solvent was removed under reduced pressure. The aqueous solution was then diluted with CH_2Cl_2 and washed three times with water. The organic phase was dried over Na_2SO_4. After the solvent was removed, the crude product was pre-purified by column chromatography with silica gel (CH_2Cl_2/MeOH: 98 : 2). Subsequently, the resulting mixed fraction was purified by flash chromatography over a RediSep® HC Duo column (gradient: CH_2Cl_2/MeOH: 100 : 0; 98 : 2; 96 : 4; 95 : 5). The product-containing test tubes were then over-poured with n-hexane to precipitate the product to obtain a dark red solid (0.017 g, 13 %). ^{1}H-NMR (500 MHz, DMSO-d_6): δ = 9.15 (d, *J* = 6.6 Hz, 1H, arom.), 9.02 (d, *J* = 8.5 Hz, 1H, arom.), 8.71 (s, 1H, arom.), 8.56 (d, *J* = 15.7 Hz, 1H, R–CH=CH–R), 8.51 (d, *J* = 16.2 Hz, 1H, R–CH=CH–R), 8.44 (d, *J* = 6.7 Hz, 1H, arom.), 8.39 (s, 1H, arom.), 8.36 (d, *J* = 8.8 Hz, 1H, arom.), 8.25–8.21 (m, 1H, arom.), 8.10 (d, *J* = 15.8 Hz, 1H, R–CH=CH–R), 8.06–8.02 (m, 1H, arom.), 7.93 (d, *J* = 8.6 Hz, 1H, arom.), 7.71 (d, *J* = 15.9, 1H, R–CH=CH–R), 7.68 (d, *J* = 3.4 Hz, 1H, arom.), 4.46 (s, 3H, R–CH_3), 3.97 (s, 3H, R–CH_3), 2.97 (s, 3H, R–CH_3). ^{13}C-NMR (126 MHz, DMSO-d_6): δ = 165.9, 164.5, 153.6, 146.8, 141.2, 138.8, 138.7, 136.9, 136.2, 134.7, 128.9, 128.7, 126.5, 126.3, 125.6, 122.7, 121.6, 119.1, 118.8, 114.3, 113.8, 113.8, 111.8, 44.0, 33.6, 20.8. HR-ESI-MS (m/z): $[M]^+$ calcd. for $C_{26}H_{23}N_6^+$: 419.1979; found: 419.1977.

1: Compound **3** (0.212 g, 0.464 mmol, 1.00 equiv.), $Pd_2(dba)_3$ (0.045 g, 0.026 mmol, 5 mol %) and QPhos (0.068 g, 0.096 mmol, 20 mol %) were added to a 10 mL crimp-vial and dried under high vacuum. The solids were then solved with dry DMF (1.00 mL). Subsequently, 2.00 mL of a 0.24 M tetrazine stock solution (**9**). and dry Et_3N (0.32 mL, 2.33 mmol, 5.00 equiv.) were added to the solution. The reaction took place in a metal heating block at 80 °C for 18 h. After the solution has cooled to r.t., the solution was mixed with an excess of an aqueous solution of KPF_6 and stirred vigorously for 15 min. The organic solvent was removed under reduced pressure. The aqueous solution was then diluted with CH_2Cl_2 and washed three times with water. The organic phase was dried over Na_2SO_4. After the solvent has been removed, the crude product was purified *via* column chromatography (CH_2Cl_2/MeOH 99 : 1, 98 : 2, 95 : 5) to obtain an orange solid (0.075 g, 31 %). ^{1}H-NMR (400 MHz, DMSO-d_6): δ = 8.94 (d, *J* = 16.0 Hz, 1H, R–CH=CH–R), 8.67 (d, *J* = 6.5 Hz, 2H, arom.), 8.32 (d, *J* = 15.9 Hz, 1H, R–CH=CH–R), 8.21 (s, 1H, arom.), 7.96 (d, *J* = 6.6 Hz, 2H, arom.), 7.75 (d, *J* = 7.4 Hz, 1H, arom.), 7.66 (d, *J* = 8.1 Hz, 1H, arom.), 7.57 (d, *J* = 16.0 Hz, 1H, R-CH=CH-R), 7.38 (t, *J* = 7.8 Hz, 1H, arom.), 7.14 (d, *J* = 15.9 Hz, 1H,

R–CH=CH–R), 4.20 (s, 3H, R–CH_3), 3.93 (s, 3H, R–CH_3), 3.00 (s, 3H, R–CH_3). ^{13}C-NMR (101 MHz, DMSO-d_6): δ = 166.1, 164.2, 153.1, 144.4, 138.2, 138.0, 135.0, 133.4, 128.6, 124.3, 122.8, 122.2, 122.0, 120.3, 118.9, 112.8, 112.7, 46.4, 33.4, 20.9. HR-ESI-MS (m/z): $[M]^+$ calcd. for $C_{22}H_{21}N_6^+$: 369.1822; found: 369.1817.

25: Under argon atmosphere, **23** (170 mg, 0.266 mmol, 1.00 eq) was dissolved in MeOH. NaOH solution (15 g dissolved in 15 mL H_2O) was added and stirred for 2 h at ambient temperature. The solvent was removed under reduced pressure and the precipitate was dried. The precipitate was redissolved in anhydrous DMF (5 mL), triethylamine (0.147 mL, 107 mg, 1.06 mmol, 4.00 eq) and **20** (100 mg, 0.398 mmol, 1.50 eq) was added and the solution was stirred at ambient temperature for 16 h. The solvent was removed under reduced pressure. The brown residue was dissolved in MeOH (20 mL) and stirred with Amberlite IRA 402 bicarbonate for 30 min. After filtration and removal of the solvent, the product was purified *via* column chromatography (CH_2Cl_2/MeOH = 50 : 1). The product was obtained as a light yellow solid (148 mg, 0.191 mmol, 72 %). ^{1}H-NMR (400 MHz, $CDCl_3$): δ = 8.03 (s, 1H), 7.99 (s, 1H), 7.40 (dd, J = 8.5, 1.3 Hz, 2H), 5.99 (d, J = 5.9 Hz, 1H), 4.88 (s, 1H), 4.21–4.19 (m, 2H), 4.15–4.10 (m, 3H), 4.05 (s, 2H), 3.94–3.91 (m, 1H), 3.76–3.73 (m, 1H), 2.88 (s, 1H), 2.48–2.46 (m, 1H), 2.25–2.19 (m, 2H), 1.89–1.84 (m, 2H), 0.97 (s, 9H), 0.91 (s, 9H), 0.86 (s, 9H), 0.17 (d, J = 4.1 Hz, 6H), 0.08 (d, J = 7.4 Hz, 6H), 0.03 (s, 3H, −0.03 (s, 3H). ^{13}C-NMR (101 MHz, $CDCl_3$): δ = 162.58, 161.30, 156.21, 149.07, 142.96, 121.70, 121.40, 99.58, 89.89, 88.21, 86.09, 76.13, 74.57, 72.19, 69.75, 62.78, 38.26, 36.50, 31.69, 27.01, 26.20, 25.81, 25.70, 21.14, 18.60, 18.08, 17.91, −4.38, −4.60, −4.73, −5.37. HR-ESI-MS (m/z): $[M]^+$ calcd. for $C_{38}H_{66}N_3O_8Si_3^+$: 776.4079 ; found: 776.4139.

12: Under argon atmosphere **25** (148 mg, 0.190 mmol, 1.00 eq) was dissolved in anhydrous THF (5 mL). $Et_3N{\cdot}3HF$ (0.335 mL) was slowly added to the solution. The mixture was stirred at ambient temperature overnight. The solvent removed under reduced pressure and the crude product was purified *via* column chromatography (CH_2Cl_2/MeOH 6 : 1). The product was obtained as a white solid (58 mg, 133 μmol, 70 %). ^{1}H-NMR (400 MHz, DMSO-d6): δ = 11.63 (s, 1H), 8.20 (s, 1H), 7.74 (s, 1H), 7.62 (s, 1H), 5.75 (d, J = 5.1 Hz, 1H), 5.39 (d, J = 5.5 Hz, 1H), 5.17 (t, J = 4.7 Hz, 1H), 5.06 (d, J = 5.2 Hz, 1H), 4.05–4.03 (m, 3H), 3.99–3.94 (m, 3H), 3.67–3.63 (m, 1H), 3.58–3.54 (m, 1H), 2.18–2.14 (m, 2H), 1.83–1.79 (m, 2H). ^{13}C-NMR (101 MHz, DMSO-d6): δ = 162.03, 156.71, 150.19, 144.24, 122.29, 121.86, 98.73, 90.50, 88.59, 85.44, 74.65, 74.23, 70.08, 68.97, 60.99, 46.20, 38.52, 31.03, 27.21, 20.56. HR-ESI-MS (m/z): $[M]^+$ calcd. for $C_{20}H_{24}N_3O_8^+$: 434.4170; found for $C_{20}H_{23}N_3O_8Na^+$: 456.1270.

26: Under argon atmosphere, **24** (170 mg, 0.266 mmol, 1.00 eq) was dissolved in MeOH. NaOH solution (15 g dissolved in 15 mL H_2O) was added and stirred for 2 h at ambient temperature. The solvent was removed under reduced pressure and the precipitate was dried. The precipitate was redissolved in anhydrous DMF (5 mL), triethylamine (0.147 mL, 107 mg, 4.00 eq) and **20** (100 mg, 0.398 mmol, 1.50 eq) was added and the reaction solution was stirred at ambient temperature for 16 h. The solvent was removed under reduced pressure. The brown residue was dissolved in MeOH (20 mL) and stirred with Amberlite IRA 402 bicarbonate for 30 min. After filtration evaporation under reduced pressure, the product was purified *via* column chromatography (CH_2Cl_2/MeOH = 50 : 1). The product was obtained as a yellow solid (78 mg, 38 %). ^{1}H-NMR (400 MHz, $CDCl_3$): δ = 7.86 (s, 1H), 7.52 (s, 1H), 7.45 (s, 1H), 7.41–7.40 (m, 2H), 6.03 (d, *J* = 6.9 Hz, 1H), 4.13–4.11 (m, 3H), 4.06–4.02 (m, 3H), 3.88–3.85 (m, 2H), 3.75–3.75 (m, 3H), 3.17 (s, 2H), 2.25–2.20 (m, 2H), 1.89–1.86 (m, 2H), 1.70–1.68 (m, 2H), 0.96 (s, 9H), 0.92 (s, 9H), 0.85 (s, 9H), 0.14 (s, 6H), 0.10 (s, 3H), 0.09 (s, 3H), 0.02 (s, 3H), −0.07 (s, 3H). ^{13}C-NMR (101 MHz, DMSO-d_6): δ = 176.73, 161.48, 149.06, 143.10, 111.88, 111.86, 99.56, 90.20, 88.27, 86.08, 77.35, 77.03, 76.71, 76.16, 74.43, 72.15, 62.75, 30.48, 26.21, 25.84, 25.81, 25.70, 22.57, 21.08, 18.60, 18.08, 17.91, −4.38, −4.60, −4.74, −5.37, −5.40. HR-ESI-MS (m/z): $[M]^+$ calc. for $C_{38}H_{69}N_3O_8Si_3^+$: 779.4392; found: $C_{38}H_{69}N_3O_8Si_3Na^+$ 802.405.

13: Under argon atmosphere **26** (78 mg, 0.190 mmol, 1.00 eq) was dissolved in anhydrous THF (5 mL) .$Et_3N{\cdot}3HF$ (0.335 mL) was added slowly to the solution. The mixture was stirred at ambient temperature for 2 d. The solvent was evaporated under reduced pressure. The crude product was purified *via* column chromatography (CH_2Cl_2/MeOH 6 : 1). The product was obtained as a slightly yellow foam (44 mg, quant.). ^{1}H-NMR (400 MHz, DMSO-d_6): δ = 11.19 (s, 1H), 7.74 (s, 1H), 7.73 (s, 1H), 7.11-7.08 (m, 1H), 5.77 (*d, J* = 5.5 Hz, 1H), 5.33 (d, *J* = 5.8 Hz, 1H), 5.07-5.05 (m, 2H), 4.09–4.04 (m, 2H, 3.99–3.95 (m, 3H), 3.83–3.81 (m, 1H), 3.63–3.61 (m, 1H), 3.57–3.53 (m, 1H), 3.17 (d, *J* = 5.2 Hz, 2H), 2.99–2.93 (m, 2H), 2.20–2.13 (m, 3H), 1.83–1.78 (m, 2H), 1.55–1.52 (m, 2H). ^{13}C-NMR (101 MHz, DMSO-d_6): δ = 163.84, 156.97, 151.12, 141.43, 137.04, 122.29, 121.89, 113.44, 88.12, 85.21, 73.76, 70.35, 68.54, 61.54, 57.27, 38.56, 28.76, 27.29, 24.16, 20.57. HR-ESI-MS (m/z): $[M]^+$ calcd. for $C_{20}H_{28}N_3O_8^+$: 438.1798; found: 438.1872.

14: Under argon atmosphere, **21** (25 mg, 81.3 μmol, 1.00 eq) was dissolved in MeOH. NaOH solution (15 g dissolved in 15 mL H_2O) was added and stirred for 2 h at ambient temperature. The solvent was removed under reduced pressure and the precipitate was dried. The precipitate was redissolved in anhydrous THF (5 mL), triethylamine (45 μL, 32.8 mg, 4.00 eq) and **20** (25 mg, 97.6 μmol, 1.20 eq) was added and the solution was stirred for 16 h at ambient temperature. The solvent was removed under reduced pressure. The brown residue was dissolved in MeOH (20 mL) and stirred with Amberlite IRA 402 bicarbonate for 30 min. After filtration and evaporation of solvent under reduced pressure, the product was purified *via* column chromatography (CH_2Cl_2/MeOH = 20 : 1). The product was obtained as a yellow solid (7 mg, 20 %) ^{1}H-NMR (400 MHz, DMSO-d_6): δ = 8.10 (s, 1H), 7.74 (s, 2H), 7.70 (s, 1H), 6.48–6.45 (m, 1H), 5.26 (s, 1H), 5.07 (s, 1H), 4.34–4.32 (m, 1H), 4.08–4.06 (m, 2H), 4.03–4.02(m, 2H), 3.82 (s, 1H), 3.58–3.55 (m, 1H), 3.51–3.48 (m, 1H), 2.19–2.14 (m, 3H), 1.84–1.80 (m, 2H). ^{13}C-NMR (101 MHz, DMSO-d_6): δ = 158.00, 157.05, 153.12, 150.03, 126.83, 122.28, 121.86, 102.85, 95.01, 89.70, 87.72, 85.70, 75.67, 74.47, 70.99, 69.03, 61.98, 38.53, 27.23, 20.57. . HR-ESI-MS (m/z): $[M]^+$ calc. for $C_{22}H_{25}N_5O_5^+$: 439.4720; found: $C_{22}H_{22}N_5O_5^+$ 436.179.

15: Under argon atmosphere, **22** (25 mg, 81.3 μmol, 1.00 eq) was dissolved in MeOH. NaOH solution (15 g dissolved in 15 mL H_2O) was added and stirred for 2 h at ambient temperature. The solvent was removed under reduced pressure and the precipitate was dried. The precipitate was redissolved in anhydrous THF (5 mL), triethylamine (45 μL, 32.8 mg, 4.00 eq) and **20** (25 mg, 97.6 μmol, 1.20 eq) was added and the solution was stirred for 16 h at ambient temperature. The solvent was removed under reduced pressure. The brown residue was dissolved in MeOH (20 mL) and stirred with Amberlite IRA 402 bicarbonate for 30 min. After filtration and evaporation of solvent under reduced pressure, the product was purified *via* column chromatography (CH_2Cl_2/MeOH = 20 : 1). The product was obtained as a yellow solid (12 mg, 33 %) ^{1}H-NMR (400 MHz, DMSO-d_6): δ = 8.01 (s, 1H), 7.74 (s, 2H), 7.17-7.15 (m, 1H), 7.10 (s, 1H), 6.55 (s, 2H), 6.48–6.44 (m, 1H), 5.21 (d, *J* = 4.1 Hz, 1H), 5.05 (t, *J* = 5.7 Hz, 1H), 4.31–4.30 (m, 1H), 4.01 (d, *J* = 7.4 Hz, 2H), 3.79–3.77 (m, 1H), 3.57–3.51 (m, 1H), 3.49–3.45 (m, 1H), 3.06–3.04 (m, 2H), 2.74–2.70 (m, 2H), 2.18–2.09 (m, 4H), 1.83–1.79 (m, 2H), 1.69–1.67 (m, 2H).). ^{13}C-NMR (101 MHz, DMSO-d_6): δ = 162.79, 158.04, 156.98, 151.77, 150.88, 122.29, 121.90, 119.19, 115.11, 102.51, 87.58, 83.19, 71.59, 68.55, 62.65, 38.59, 36.25, 31.24, 30.92, 27.30, 23.64, 20.58. HR-ESI-MS (m/z): $[M]^+$ calc. for $C_{22}H_{28}N_5O_5^-$: 443.212; found: $C_{22}H_{28}N_5O_5^-$ 443.212.

DNA1 and **DNA2**: According to literature, DNA was synthesized *via* a DNA synthesizer.[10] Oligonucleotides were synthesized by using standard solid-phase phosphoramidite synthesis protocol on a H-6 DNA/RNA synthesizer by K&A Laborgeräte. Controlled Pore Glass (CPG) was used as a solid phase with an occupancy of 1 μmol (500 Å). Phosphoramidites of 2′-deoxyadenosine, 2′-deoxyguanosine, 2′-deoxycytidine, thymidine were purchased from Sigma Aldrich.and were used as a 67 mM solution in acetonitrile. Phosphoramidites **27** or **28** were used as a 100 mM solution in CH_2Cl_2. After synthesis, the CPG columns were dried in high vacuum and the resin was removed from the columns and transferred to an Eppendorf reaction vial. 700 μL of 25% aq. NH_4OH was added and the suspension incubated over night at 55 °C, followed by removal of the solvents by vacuum centrifugation (35 min, 35 °C, 100 mbar, followed by 4 h, 25 °C, 0.100 mbar). The crude product was purified by a standard Glen Gel-Pak™ desalting protocol. MALDI-TOF with 3-HPA as a matrix substance: calcd. for **DNA2** $[M]^+$: 5213.92, found $[M+H]^+$: 5214.38; calcd. for **DNA1** $[M]^+$: 5209.89, found $[M+H]^+$: 5210.06;

DNA3-DNA6: Approximately 1 μmol of **DNA1** and **DNA2** was dissolved in anhydrous DMSO (300 μL). NHS ester **20 or 49** (2 mg) was dissolved in anhydrous DMSO (100 μL) and added to the corresponding DNA solution. $(i\text{Pr})_2\text{NEt}$ (5 μL) was added and the vials were shook on a laboratory shaker for 16 h. After completion of the reaction, the solvent was removed in the vacuum centrifuge (8 h, 25 °C, 0.100 mbar). The DNA pellet was dissolved in water (600 μL) and purified via semi-preparative HPLC VDSpher OptiBio PUR 300 S18-SE column (250×10 mm, 5 μm, 300 μL injection, 0–20% acetonitrile, 0.1 M NH_4OAc, 40 °C, 30 min). The detection wavelength was set to 260 and 280 nm. MALDI-TOF with 3-HPA as a matrix substance: calcd. for **DNA3** $[M]^+$: 5346.6, found $[M]^+$:5346.6. calcd. for **DNA4** $[M]^+$: 5350.2, found $[M-H]^+$: 5348.2; calcd. for **DNA5** $[M]^+$: 5390.04, found $[M+H]^+$: 5393.02; calcd. for **DNA6** $[M]^+$: 5385.97, found $[M+H]^+$: 5389.35. For annealing, the modified oligonucleotide (10 μM) was heated together with 1.20 equiv. of the corresponding complementary oligonucleotide in 10 mM NaP_i buffer (pH 7) and 250 mM NaCl solution to 90 °C for 10 min and then slowly cooled to r.t. over night.

Acknowledgements

Financial support by the Deutsche Forschungsgemeinschaft (grants Wa 1386/17-2, Wa 1386/22-1 and GRK 2039/2) and by the KIT are gratefully acknowledged. Open Access funding enabled and organized by Projekt DEAL.

Conflict of Interests

The authors declare no conflict of interest.

Data Availability Statement

The data that support the findings of this study are available in the supplementary material of this article.

Keywords: bicyclononyne · spirohexene · oligonucleotide · Diels-Alder reaction

[1] a) H. Wu, N. K. Devaraj, *Acc. Chem. Res.* **2018**, *51*, 1249–1259; b) N. K. Devaraj, R. Weissleder, S. A. Hilderbrand, *Bioconjugate Chem.* **2008**, *19*, 2297–2299.
[2] a) K. Lang, J. W. Chin, *ACS Chem. Biol.* **2014**, *9*, 16–20; b) S. Mayer, K. Lang, *Synthesis* **2017**, *49*, 830–848.
[3] a) E. Kozma, P. Kele, *Org. Biomol. Chem.* **2019**, *17*, 215–233; b) N. K. Devaraj, S. Hilderbrand, R. Upadhyay, R. Mazitschek, R. Weissleder, *Angew. Chem. Int. Ed.* **2010**, *49*, 2869–2872; c) A. Spampinato, E. Kuzmová, R. Pohl, V. Sýkorová, M. Vrábel, T. Kraus, M. Hocek, *Bioconjugate Chem.* **2023**, *34*, 772–780; d) A. Wieczorek, T. Buckup, R. Wombacher, *Org. Biomol. Chem.* **2014**, *12*, 4177–4185; e) P. Werther, J. S. Möhler, R. Wombacher, *Chem. Eur. J.* **2017**, *23*, 18216–18224.
[4] A. Nadler, C. Schultz, *Angew. Chem. Int. Ed.* **2013**, *52*, 2408–2410.
[5] a) F. Hild, P. Werther, K. Yserentant, R. Wombacher, D.-P. Herten, *Biophys. Rep.* **2022**, *2*, 100084; b) B. Pinto-Pacheco, W. P. Carbery, S. Khan, D. B. Turner, D. Buccella, *Angew. Chem. Int. Ed.* **2020**, *59*, 22140–22149.
[6] J. C. T. Carlson, L. G. Meimetis, S. A. Hilderbrand, R. Weissleder, *Angew. Chem. Int. Ed.* **2013**, *52*, 6917–6920.
[7] P. Werther, K. Yserentant, F. Braun, K. Grußmayer, V. Navikas, M. Yu, Z. Zhang, M. J. Ziegler, C. Mayer, A. J. Gralak, M. Busch, W. Chi, F. Rominger, A. Radenovic, X. Liu, E. A. Lemke, T. Buckup, D.-P. Herten, R. Wombacher, *ACS Cent. Sci.* **2021**, *7*, 1561–1571.
[8] J. Galeta, R. Dzijak, J. Oboril, M. Dracinský, M. Vrabel, *Chem. Eur. J.* **2020**, *26*, 9945–9953.
[9] W. Mao, W. Chi, X. He, C. Wang, X. Wang, H. Yang, X. Liu, H. Wu, *Angew. Chem. Int. Ed.* **2022**, *61*, e202117386.
[10] E. Albitz, K. Németh, G. Knorr, P. Kele, *Org. Biomol. Chem.* **2023**, *21*, 7358–7366.
[11] M. Auvray, D. Naud-Martin, G. Fontaine, F. Bolze, G. Clavier, F. Mahuteau-Betzer, *Chem. Sci.* **2023**, *14*, 8119–8128.
[12] M. O. Loehr, N. W. Luedtke, *Angew. Chem. Int. Ed.* **2022**, *61*, e202112931.
[13] P. Geng, E. List, F. Rönicke, H.-A. Wagenknecht, *Chem. Eur. J.* **2023**, *29*, e202203156.
[14] a) Z. Yu, T. Ohulchanskyy, P. An, P. N. Prasad, Q. Lin, *J. Am. Chem. Soc.* **2013**, *135*, 16766–16769; b) C. P. Ramil, M. Dong, P. An, T. M. Lewandowski, Z. Yu, L. J. Miller, Q. Lin, *J. Am. Chem. Soc.* **2017**, *139*, 13376–13386.
[15] G. Knorr, E. Kozma, A. Herner, E. A. Lemke, P. Kele, *Chem. Eur. J.* **2016**, *22*, 8972–8979.
[16] U. Rieder, N. W. Luedtke, *Angew. Chem. Int. Ed.* **2014**, *53*, 9168–9172.

Manuscript received: October 27, 2023
Revised manuscript received: November 29, 2023
Accepted manuscript online: December 5, 2023
Version of record online: ■■, ■■

RESEARCH ARTICLE

High Turn-on and fast kinetics! The inverse electron demand Diels-Alder reactions of the synthesized yellow and red tetrazine-modified dyes with spirohexene-modified nucleosides and DNA provide large Stokes-shifts with high quantum yields. With no washing steps, cell imaging could be performed. We introduce two completely new dyes and spirohexene modfied compounds which extend the toolbox of already existing clickable modifications.

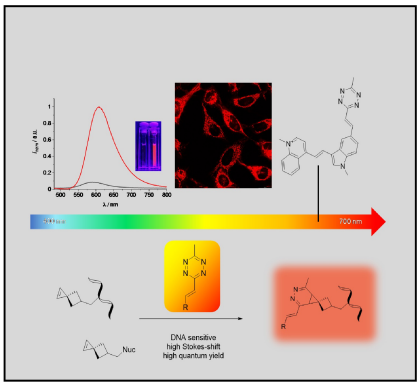

*B. Pfeuffer, Dr. P. Geng, Prof. Dr. H.-A. Wagenknecht**